THE JOURNAL OF BIOLOGICAL CHEMISTRY
Vol. 279, No. 41, Issue of October 8, pp. 42516–42527, 2004

A Gain of Function Mutation in the Activation Loop of Platelet-derived Growth Factor β-Receptor Deregulates Its Kinase Activity*[S]

Received for publication, June 1, 2004, and in revised form, July 26, 2004
Published, JBC Papers in Press, July 28, 2004, DOI 10.1074/jbc.M406051200

Federica Chiara‡, Marie-José Goumans§, Henrik Forsberg‡¶, Aive Ahgrén‡, Andrea Rasola‖, Pontus Aspenström‡, Christer Wernstedt‡, Carina Hellberg‡, Carl-Henrik Heldin‡, and Rainer Heuchel‡**

From the ‡Ludwig Institute for Cancer Research, Box 595, Uppsala S-751 24, Sweden, §Hart Long Centrum Utrecht Cardiology, Laboratory Experimental Cardiology, AZU, Heidelberglaan 100, Utrecht 3584 CX, The Netherlands, and ‖Institute for Cancer Research and Treatment, Division of Molecular Oncology, University of Torino Medical School, Strada Provinciale 142, km 3.95, Candiolo (Torino) I-10060, Italy

The platelet-derived growth factor receptors (PDGFRs) are receptor tyrosine kinases implicated in multiple aspects of cell growth, differentiation, and survival. Recently, a gain of function mutation in the activation loop of the human PDGFRα has been found in patients with gastrointestinal stromal tumors. Here we show that a mutation in the corresponding codon in the activation loop of the murine PDGFRβ, namely an exchange of asparagine for aspartic acid at amino acid position 849 (D849N), confers transforming characteristics to embryonic fibroblasts from mutant mice, generated by a knock-in strategy. By comparing the enzymatic properties of the wild-type *versus* the mutant receptor protein, we demonstrate that the D849N mutation lowers the threshold for kinase activation, causes a dramatic alteration in the pattern of tyrosine phosphorylation kinetics following ligand stimulation, and induces a ligand-independent phosphorylation of several tyrosine residues. These changes result in deregulated recruitment of specific signal transducers. The GTPase-activating protein for Ras (RasGAP), a negative regulator of the Ras mitogenic pathway, displayed a delayed binding to the mutant receptor. Moreover, we have observed enhanced ligand-independent ERK1/2 activation and an increased proliferation of mutant cells. The p85 regulatory subunit of the phosphatidylinositol 3′-kinase was constitutively associated with the mutant receptor, and this ligand-independent activation of the phosphatidylinositol 3′-kinase pathway may explain the observed strong protection against apoptosis and increased motility in cellular wounding assays. Our findings support a model whereby an activating point mutation results in a deregulated PDGFRβ with oncogenic predisposition.

The platelet-derived growth factor receptors (PDGFRs)[1] belong to the receptor tyrosine kinase superfamily and are involved in regulating essential cell processes such as cell proliferation, motility, and survival (1). There are two structurally related PDGF receptors; the α- and β-receptor each contain a large extracellular domain involved in growth factor binding and an intracellular region including a kinase domain. Growth factor binding induces receptor homo- or heterodimerization at the plasma membrane, which leads to the activation of the intrinsic kinase activity. This results in the autophosphorylation of a number of tyrosine residues in the intracellular domain, which in turn act as docking sites for downstream signaling proteins containing phosphotyrosine recognition domains (2, 3).

PDGFRs can become potent oncoproteins when they are overexpressed or mutated (reviewed in Refs. 4 and 5). Recently, PDGFRα-activating mutations were found in patients with gastrointestinal stromal tumors (6–12). One of these mutations, the substitution of valine for the highly conserved aspartic acid in the activation loop of PDGF β-receptor (PDGFRβ), is homologous to those found in other receptor tyrosine kinases such as Kit, Fms-related tyrosine kinase 3 (Flt3), and Met; these mutations cause human diseases such as mast cell disorders and germ cell tumors, acute myeloid leukemia, and papillary renal carcinomas, respectively (6).

The molecular mechanisms coupling these biochemical alterations to the oncogenic properties of the mutant receptors are unclear. Structural and biochemical studies have revealed that receptor tyrosine kinases are allosteric enzymes in equilibrium between active and inactive states. Oncogenic mutations up-regulate the tyrosine kinase activity, possibly by inducing a dynamic imbalance in favor of the active conformation of the kinase. Evidence for this molecular mechanism is provided by a recent analysis of similar mutations in the Met receptor causing human papillary renal carcinomas. In this case, the mutations D1228N or D1228H decrease the threshold of activation, since they overcome the requirement for the phosphorylation of one of the two tyrosines in the activation loop essential for wild-type receptor activation (13).

In the present work, we demonstrate that replacement of the aspartic acid with asparagine in the activation loop of the PDGFRβ kinase domain in a position corresponding to oncogenic mutations in other receptor tyrosine kinases alters the phosphorylation kinetics of several tyrosine residues that are binding sites for downstream molecules such as RasGAP or phosphatidylinositol 3′-kinase (PI3K). As a result, the D849N mutant PDGFRβ up-regulates antiapoptotic pathways, in-

* The costs of publication of this article were defrayed in part by the payment of page charges. This article must therefore be hereby marked "*advertisement*" in accordance with 18 U.S.C. Section 1734 solely to indicate this fact.

[S] The on-line version of this article (available at http://www.jbc.org) contains two additional figures.

¶ Supported by a European Union grant (second generation of transgenic models for human diseases).

** To whom correspondence should be addressed. Tel.: 46-18-160409; Fax: 46-18-160420; E-mail: Rainer.Heuchel@licr.uu.se.

[1] The abbreviations used are: PDGFR, platelet-derived growth factor receptor; PDGF, platelet-derived growth factor; PI3K, phosphatidylinositol 3′-kinase; ES, embryonic stem; MEF, mouse embryonic fibroblast; FCS, fetal calf serum; PBS, phosphate-buffered saline; TRITC, tetramethylrhodamine isothiocyanate; ERK, extracellular signal-regulated kinase; STS, staurosporine.

creases cellular transforming capacity *in vitro*, and leads to alterations in cell motility and proliferation.

EXPERIMENTAL PROCEDURES

Generation of Mutant Mice—The genomic DNA used as homology arms in the targeting vector was cut out of genomic subclones prepared previously (14). The mutation of aspartic acid 849 to asparagine was introduced into subcloned genomic DNA by oligonucleotide-directed mutagenesis using the QuikChange kit (Stratagene) according to the manufacturer's recommendations. The mutation primers were as follows: 5′-GACTTCGGCCTGGCTCGAaATATTATGAGGGACTCAAACTACA-3′ and 5′-TGTAGTTTGAGTCCCTCATAATATtTCGAGCCAGGCCGAAGTC-3′ (base exchange resulting in amino acid mutation indicated in lowercase letters). The mutation was finally confirmed by sequencing of a PCR-amplified DNA fragment from targeted embryonic stem (ES) cells.

The targeting vector consisted of a 1.7-kb EcoRV-SpeI genomic 5′-fragment, followed by a PGKneobpA expression cassette flanked by loxP sites, a 5-kb SpeI-XhoI genomic 3′-fragment containing the point mutated exon 18, and a herpes simplex virus thymidine kinase expression cassette in pBluescript SK(+). The construct was linearized (NotI) for electroporation into R1-ES cells (15), and colonies were selected with G418 and gancyclovir. Homologous recombination events were screened by PCR, as described (14), using primers for the *neo* gene (5′-TGGCTACCCGTGATATTGCT-3) and genomic sequence outside the targeting construct (5-CCGAAATGTGTACCAGTCTGAAA-3), resulting in a 3-kb amplification product for correct integration. Positive ES cell clones were tested by Southern blot, as described (14), using a 177-bp PCR amplification product corresponding to nucleotides 1957–2133 of the mouse PDGFRβ cDNA, which hybridizes to genomic DNA 5′ outside of the targeting construct (5.2-kb wild-type allele; 6.9-kb mutant allele). Coat chimeras using ES-cell clone 1B11 were generated by morula aggregation, as described previously (16). The *neo* cassette was not removed, since its presence at that specific position in intron 15 had been shown previously to be without effect on the expression of the PDGFRβ (14, 17).

Mouse Embryonic Fibroblasts (MEFs)—3T3-like embryonic fibroblasts were derived from E13 embryos (129Sv/C57Bl/6 mixed background) according to standard procedures (18). Cells were grown in Dulbecco's modified Eagle's medium (Invitrogen) supplemented with 10% fetal bovine serum (Sigma), 0.1 mM β-mercaptoethanol, 2 mM L-glutamine. All experiments involving mouse embryonic fibroblasts were done repeatedly with two or more cell isolates to exclude clonal variation.

Plasmids, Cell Culture, and Transfection—Site-directed mutagenesis was performed on a cDNA encoding the full-length human PDGFRβ inserted into the pcDNA3 expression vector (Invitrogen), using the QuikChange kit (Stratagene, La Jolla, CA). The introduced mutations were confirmed by sequencing. NIH3T3 fibroblasts were cultured in Dulbecco's modified Eagle's medium supplemented with 10% fetal bovine serum (Sigma).

Transient transfection of NIH3T3 cells was performed using a DNA-calcium phosphate procedure (CellPhect transfection kit; Amersham Biosciences) according to the manufacturer's instructions. PDGF-BB stimulation on serum-starved COS or PAE cells was performed for 7 min at 37 °C using 10 ng/ml PDGF-BB.

Focus Forming Assays—Focus forming assays were performed as described (13). Briefly, NIH3T3 cells (1.5×10^5 cells/10-cm dish) were transfected with the appropriate pcDNA3 plasmid (10 μg/dish) by the calcium phosphate method in the presence of 10% calf serum. After 24 h, the serum concentration was reduced to 5%, and cells were cultured for an additional 21 days. Foci were scored following staining with Giemsa dye.

Immunoprecipitation and Immunoblotting—Protein extracts were obtained by lysing cells in EB buffer (100 mM Tris-HCl, pH 7.4, 150 mM NaCl, 1% Triton X-100, 10% glycerol) in the presence of 1 mM sodium orthovanadate and protease inhibitors. Extracts were clarified by centrifugation, and protein concentration was determined by the BCA protein assay system (Pierce).

PDGFRβ was immunoprecipitated from cell lysates (~1 mg of lysate protein) using 2 μg of antibody plus 20 μl of Protein A-Sepharose beads at 4 °C for 2 h. The beads were then washed two times with EB buffer and two times with TBS buffer (20 mM Tris-HCl, pH 7.5, 5 mM EDTA, 150 mM NaCl), boiled for 5 min in 2× Laemmli sample buffer, and run on an SDS 8–12% gradient polyacrylamide gel. Proteins were then transferred to nitrocellulose membranes at 100 V for 2 h and probed with anti-phosphotyrosine antibodies or anti-PDGFRβ antibodies. Antisera against Tyr(P), PDGFRβ (sc958), and GTPase-activating protein for Ras (RasGAP) were obtained from Santa Cruz Biotechnology, Inc. (Santa Cruz, CA); antisera against phospho-Akt, Akt, and phospho-ERK1/2 were purchased from Cell Signaling Technology; and the p85 subunit of PI3K antiserum was from Upstate Biotechnology, Inc. (Lake Placid, NY).

Antibodies against phosphorylated tyrosines $Tyr(P)^{579}$, $Tyr(P)^{751}$, $Tyr(P)^{771}$, and $Tyr(P)^{1021}$ of the human PDGFRβ have been described recently (19). In addition, we have validated specific antibodies against $Tyr(P)^{763}$ and $Tyr(P)^{1009}$ using wheat germ agglutinin pull-downs from lysates prepared from PAE cells transfected with either wild-type PDGFRβ or a PDGF β-receptor mutated at the respective amino acid. The site-specific antibodies yielded a specific signal only for wild-type receptors after stimulation by ligand (Supplemental Fig. 1).

Kinase Assays—For kinase assays, MEFs were lysed in the absence of sodium orthovanadate to allow dephosphorylation, and the various PDGFRβ proteins were immunoprecipitated with anti-PDGFRβ antibodies. Immunopurified proteins were then washed three times with EB buffer and two times with kinase buffer (25 mM HEPES, pH 7.1, 5 mM $MgCl_2$, 100 mM NaCl). For preactivation, 100 ng/ml PDGF-BB was added on ice for 30 min. The phosphorylation reaction was performed in kinase buffer with [γ-^{32}P]ATP (5 μCi/sample) and 10 μM unlabeled ATP for increasing time periods at room temperature. The reaction was stopped by the addition of boiling SDS-sample buffer. The samples were analyzed by 4–12% gradient SDS-PAGE and Western immunoblotting with anti-PDGFRβ antibodies, followed by quantification of radioactivity using a phosphor imager (Fuji).

Exogenous Substrate Phosphorylation Assay—The phosphorylation reaction was performed in kinase buffer in the presence of increasing concentrations of myelin basic protein, 10 μM unlabeled ATP, and [γ-^{32}P]ATP (5 μCi/sample) for 15 min at 4 °C. The reaction was stopped by the addition of EDTA. The samples were separated on an 8–12% gradient SDS-PAGE and then subjected to immunoblotting with anti-PDGFRβ antibodies and analysis by PhosphorImager analysis.

Mitogenesis Assay—MEFs were seeded in 12-well plates and grown for 24 h. The medium was then changed to starvation medium (Dulbecco's modified Eagle's medium supplemented by 1% FCS), and after 24 h, 0.2 μCi/ml [^{3}H]thymidine (Amersham Biosciences) and PDGF (0–25 ng/ml) or 10% FCS were added, and the incubation was continued for 20 h. Incorporated radioactivity was precipitated using 5% trichloroacetic acid and then dissolved in 1 M NaOH. After neutralization, incorporated radioactivity was determined in a liquid scintillation counter.

Cellular Wounding Assay—Confluent MEF cultures were grown in 6-well plates on coverslips coated with 0.1% gelatin and starved for 2 days in medium containing 0.05% serum. "Wounds" (three/glass) were introduced by scratching the coverslips with a 200-μl pipette tip. The assay was performed in the presence of 10 μg of mitomycin C/ml to inhibit proliferation. Phase-contrast microscopic pictures were taken at the indicated time points.

Fluorescence Microscopy—MEFs on coverslips were grown and "wounded" as in the cellular wounding assay. The cells were fixed in 3% paraformaldehyde in phosphate-buffered saline (PBS) at 37 °C for 25 min and washed with PBS. Then cells were permeabilized in 0.2% Triton X-100 in PBS for 5 min, washed again in PBS, and incubated in 5% fetal bovine serum in PBS for 30 min at room temperature. To visualize the filamentous actin, the cells were incubated with TRITC-conjugated phalloidin. The coverslips were mounted on object slides by the use of Fluoromount-G (Southern Biotechnology Associates). Cells were photographed by a Hamamatsu ORCA CCD digital camera employing the QED Imaging System software using a Zeiss Axioplan2 microscope.

Flow Cytometry Analysis of Apoptosis Induction—Flow cytometry recordings of several independent apoptotic changes were simultaneously performed by a single tube analysis, as described (20). Briefly, after induction of apoptosis, cells were resuspended in HEPES buffer (10 mM HEPES, 135 mM NaCl, 5 mM $CaCl_2$) and incubated for 15 min at 37 °C in fluorescein isothiocyanate-conjugated annexin V, tetramethylrhodamine methyl ester (200 nM), and propidium iodide (1 mg/ml), to detect phosphatidylserine exposure on the cell surface, mitochondrial inner membrane electrochemical gradient ($\Delta\Psi_m$), and plasma membrane integrity, respectively. Cell morphology changes were analyzed following variations of the forward and side light scatter. Samples were analyzed on a FACSCalibur flow cytometer (BD Biosciences). Data acquisition was performed using CellQuest software, and data analysis was performed with WinMDI software.

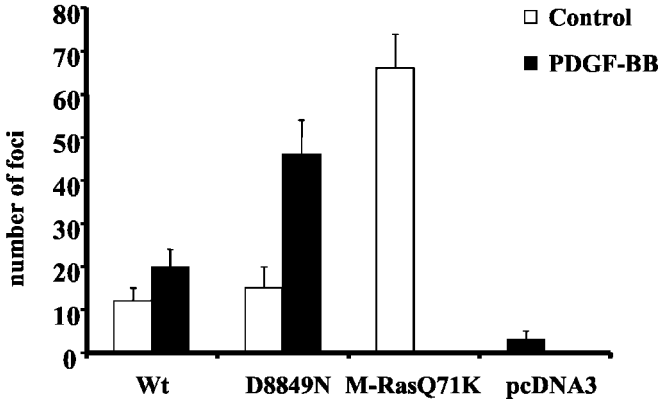

FIG. 1. **D849N mutation in the PDGFRβ activation loop confers increased transforming ability upon PDGF-BB stimulation.** NIH3T3 cells were transfected with the indicated receptor alone (*open bars*), or co-transfected with a PDGF-B expression plasmid (*closed bars*). Cells were then grown in medium containing 5% calf serum for 3 weeks, after which they were fixed and stained. The number of foci was scored for each 10-cm dish. Transfection with oncogenic Ras or empty expression vector were used as positive and negative controls, respectively.

RESULTS

An Activation Loop Mutation in the Human PDGFRβ Gives the Receptor Transforming Properties in the Presence of Ligand—It was recently shown that mutations of a highly conserved aspartic acid residue in the activation loop of Kit and Met receptors caused up-regulation of their enzymatic activity, resulting in increased transforming potential (7, 21).

To investigate the effect of this type of mutation in the human PDGFR, we generated an expression vector for human PDGFRβ harboring an aspartic acid to asparagine mutation at amino acid position 850 (D850N; corresponding to position 849 in the mouse receptor) in the activation loop of the kinase domain. Overexpression of the D850N mutant human PDGFRβ in COS cells resulted in significantly increased ligand-independent autophosphorylation (data not shown), as has been described for other tyrosine kinase receptors carrying similar mutations (22). Next, we employed NIH3T3 cells in a focus formation assay in order to compare the transforming potential of the wild-type and the mutant PDGFRβ. Each receptor type plasmid was transfected alone or in combination with a plasmid encoding the PDGF-B ligand, thus creating an autocrine stimulation loop. Cotransfection of wild-type PDGFRβ with PDGF-B gave rise to a moderate number of foci (Fig. 1). In the absence of ligand, the number of foci generated from D850N mutant cells was comparable with that from wild-type cells, whereas the coexpression of ligand significantly increased the number of foci from D850N mutant PDGFRβ cells.

Generation of Mutant Mice—The observation that the mutation in the activation loop of the PDGFRβ increased the receptor's transforming ability prompted us to generate a potential mouse tumor model by introducing this point mutation via a knock-in approach.

The genomic arms necessary for homologous recombination in ES cells were cloned into a double selection targeting vector. The wild-type exon 17, containing aspartic acid 849 (the mouse PDGFRβ is one amino acid residue shorter; thus, Asp^{849} corresponds to Asp^{850} in the human receptor) was replaced with a mutated version with the aspartic acid replaced by an asparagine residue (D849N) (Fig. 2). After electroporation of R1-ES cells (15), G418-resistant clones were screened for homologous recombination by PCR. Positive clones were subsequently verified by Southern blot analysis, and DNA sequencing of the mutant allele was performed to ensure the presence of the point mutation (data not shown). One positive ES cell clone was used to generate germ line transmitters. Heterozygous offspring showed no obvious phenotype and were intercrossed to generate homozygous offspring, which were recovered in expected Mendelian proportions (data not shown), indicating that the mutation introduced was compatible with embryonic development. We have not found any signs of tumors or fibrotic developments in mice 1 year of age, independent of the genotype.

The D849N Mutant PDGFRβ Displays an Increased Phosphorylation and Is More Sensitive to Lower Ligand Concentrations—Based on the significantly increased transforming potential of the D849N mutation in the focus formation assay, the lack of an overt phenotype even in homozygous mutant mice came as a surprise. We therefore decided to compare the characteristics of the wild-type and the D849N mutant PDGFRβ from MEFs, a cell type that normally expresses the PDGFRβ.

We first examined the ligand-dependent phosphorylation kinetics of wild-type receptor and D849N mutant PDGFRβ in a physiological context. We subjected wild-type and mutant MEFs to increasing time periods of ligand stimulation. Receptors were immunopurified, separated by SDS-PAGE, and analyzed with antibodies against phosphotyrosine or against PDGFRβ (Fig. 3*A*, *upper* and *lower panels*, respectively). Analysis of the Western blot in Fig. 3*A* revealed that the wild-type receptor was maximally autophosphorylated after 5 min of stimulation, which then quickly decreased until 60 min. The D849N mutant receptor, however, displayed not only an increased basal tyrosine phosphorylation in the absence of ligand stimulation but also an increased and prolonged ligand-stimulated tyrosine phosphorylation compared with wild-type cells. Since we did not detect any significant difference in receptor amounts, we excluded the possibility that the increased phosphorylation of the D849N mutant was due to decreased receptor degradation. In addition, we found that the D849N mutant receptor was more sensitive to lower ligand concentrations compared with the wild-type receptor (Fig. 3*B*). These results indicated that the D849N point mutation in the PDGFRβ activation loop gave rise to basal constitutive receptor activation in absence of ligand, a higher sensitivity toward lower ligand concentrations and to a more robust ligand-dependent receptor phosphorylation.

The D849N Mutation Increases the Threshold of Kinase Activation of the Receptor—We next analyzed the effects of this mutation on the autoactivation and catalytic properties of the PDGFRβ. To this end, we performed *in vitro* autophosphorylation assays on immunopurified receptors from lysates of wild-type and mutant MEFs in the presence of [γ-^{32}P]ATP. As illustrated in Fig. 4*A*, the unstimulated receptor harboring the D849N mutation was autophosphorylated at a high rate and reached full activation after 20 min of reaction at 20 °C, whereas the wild-type PDGFRβ was phosphorylated more slowly (Fig. 4*A*). The increased autoactivation velocity of the mutant receptor was observed only in the absence of the ligand. Ligand-dimerized wild-type and mutant receptors, had comparable kinetics of autoactivation (Fig. 4*B*). These data are compatible with a scenario in which mutant PDGFRs, in the absence of ligand-induced dimerization, display higher kinase activity than wild-type PDGFRβ.

To further characterize the mutant receptors, their *in vitro* kinase activities were measured in the presence of the exogenous substrate myelin basic protein. Fig. 5*A* shows that the extent of myelin basic protein phosphorylation was higher by the unstimulated D849N mutant receptor compared with the wild-type receptor. Again, after PDGF-BB stimulation, there

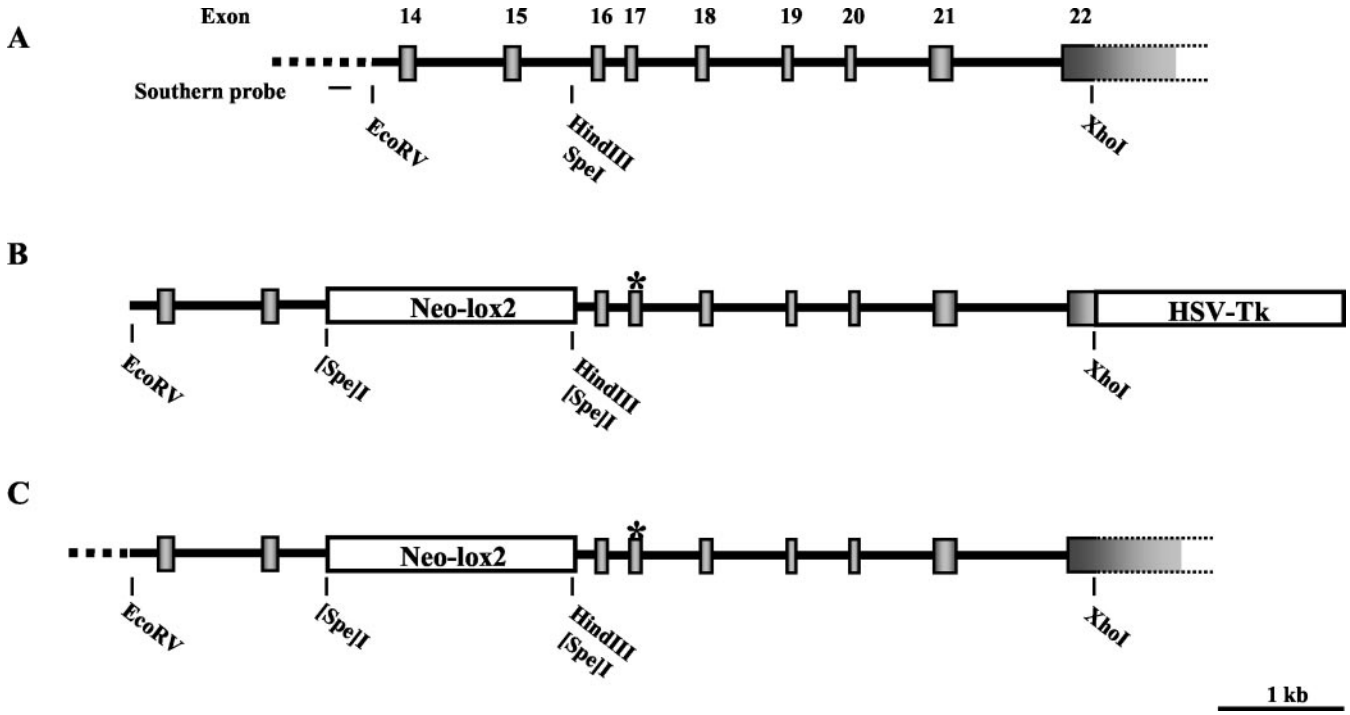

FIG. 2. **Introduction of a point mutation into the PDGFRβ.** The intron/exon structure of the mouse PDGFRβ is schematically represented, before (*A*) and after (*C*) the targeting event. *B*, the targeting vector with the genomic arms and the two selection cassettes is shown. The *asterisk* indicates the position of the D849N point mutation.

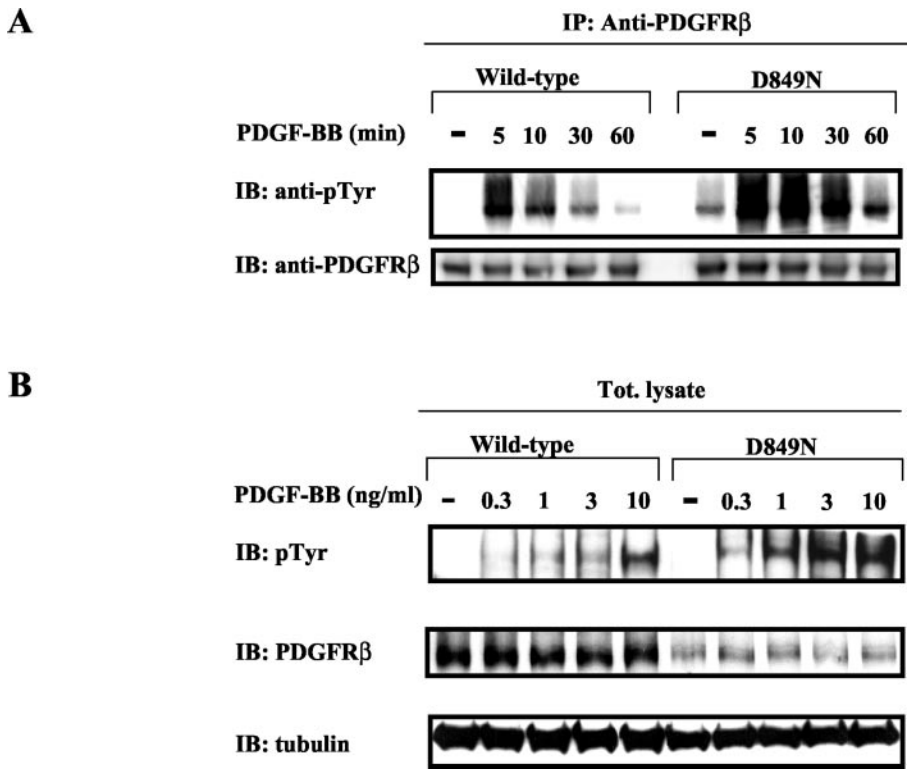

FIG. 3. **Introduction of the D849N mutation into the activation loop upregulates the PDGFRβ phosphorylation.** Wild-type or mutant PDGFRβ were immunoprecipitated (*IP*) from MEFs, either starved for 2 days and stimulated with PDGF-BB for different time periods (*A*) or starved for 3 days and stimulated with increasing amounts of PDGF-BB (*B*). Immunoprecipitated proteins were separated by SDS-PAGE, using a 4–12% gradient polyacrylamide gel, and analyzed by Western blot (*IB*) using anti-phosphotyrosine (*upper panel*) and anti-PDGFRβ antibodies (*lower panel*) to determine the relative amounts of PDGFRβ tyrosine phosphorylation.

was no difference between the wild-type and D849N mutant receptors in the phosphorylation rate (Fig. 5*B*).

Tyr^{856} in the Activation Loop of the D849N Mutant PDGFRβ Is Phosphorylated in the Absence of Ligand—Activation loop trans-phosphorylation is a general mechanism of catalytic enhancement in tyrosine kinase receptors. This event induces a conformational change of the activation loop, which moves from a conformation not optimal for phosphoryl transfer to a catalytically competent configuration. Phosphorylation of Tyr^{856} in the putative kinase activation loop has been shown to be required for full activation of PDGFRβ (23). Introduction of a mutation homologous to D849N in the activation loop of the Met receptor has been found to decrease the threshold of kinase activation, perhaps by promoting the active conformation of the activation loop (13).

To study the effects of the D849N mutation on the phosphorylation of Tyr^{856}, we developed antibodies specific for the phosphorylated form of the activation loop of the PDGFRβ. The

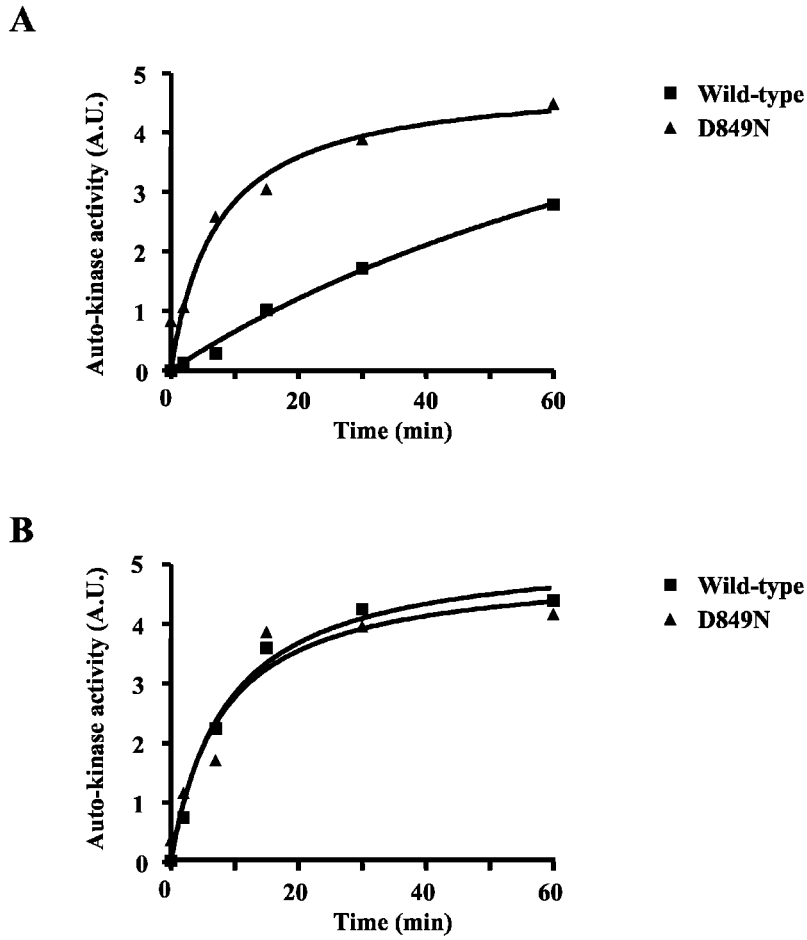

FIG. 4. **Introduction of the D849N mutation into the activation loop increases PDGFRβ autokinase activity in the absence of ligand.** MEFs from wild-type or mutant mice were starved for 1 day in medium containing 0.1% BSA and lysed in the absence of sodium orthovanadate. Immunopurified receptors were either left untreated (*A*) or stimulated with 100 ng/ml PDGF-BB (*B*), followed by incubation in the presence of [γ-^{32}P]ATP for increasing time periods. The extent of autophosphorylation was determined by SDS-PAGE and PhosphorImager analysis. Total amounts of receptor were determined by Western blotting and used to normalize the phosphor imager values. The average of two independent experiments is shown. *A.U.*, arbitrary units.

specificity of affinity-purified antibodies was analyzed by Western blotting using COS cells transiently expressing human wild-type PDGFRβ as well as mutant receptors lacking the tyrosine corresponding to mouse Tyr^{856} (Y857F) or devoid of kinase activity (K634A) as controls. As shown in Fig. 6*A*, the antibody recognized phosphorylated wild-type PDGFRβ but did not react with Y857F or K634A mutant receptors, demonstrating that the antibody specifically recognized PDGFRβ phosphorylated on Tyr^{857}.

Wild-type and D849N mutant PDGFRβ immunoprecipitated from unstimulated or ligand-stimulated MEFs were analyzed by Western blotting using the specific antibody against the phosphorylated Tyr^{856} (Fig. 6*B*, *pTyr856*). The activation loop tyrosine of the D849N mutant receptor was found to be substantially phosphorylated even in absence of ligand, whereas the wild-type receptor was phosphorylated only following ligand stimulation.

Phosphospecific Antibodies Revealed Deregulated Phosphorylation of Several Individual Autophosphorylation Sites in the D849N Mutant PDGFRβ—After we had detected significant differences not only in the total tyrosine phosphorylation, but also in the activation loop tyrosine phosphorylation, we were interested to investigate whether the D849N mutation also influences other individual tyrosine phosphorylation sites, using different site-specific, phosphotyrosine antibodies.

MEFs were subjected to prolonged starvation (48 h) in order to decrease the ligand-independent phosphorylation detected in the D849N mutant PDGFRβ and treated for different time periods with PDGF-BB. Immunopurified wild-type and mutant receptors were analyzed using specific antibodies directed against phosphorylated tyrosine residues 578, 770, 762/1008, 750, and 1020 (*i.e.* binding sites for the tyrosine kinase Src, RasGAP, the tyrosine phosphatase Shp-2, PI3K, and phospholipase C-γ, respectively). The phosphorylation kinetics of Tyr^{578}, Tyr^{1008}, Tyr^{750}, and Tyr^{1020} were comparable in both wild-type and D849N mutant receptor with the phosphorylation maximum at 5 min of stimulation, followed by a gradual decrease (Fig. 7, *A*, *C*, and *D*). However, despite a 48-h starvation, the D849N mutant PDGFRβ, but not the wild-type receptor, still displayed a basal, ligand-independent phosphorylation at all tyrosine residues tested, except for Tyr^{1008} and Tyr^{762} (Fig. 7*A*). In addition, the phosphorylation kinetics of Tyr^{770} and of Tyr^{762} were markedly changed in the D849N mutant PDGFRβ (Fig. 7, *A* and *B*). In the wild-type receptor, both Tyr^{770} and Tyr^{762} followed the global tyrosine phosphorylation pattern; conversely, in the mutant receptor, Tyr^{770} was maximally phosphorylated at 60 min (longest stimulation tested), whereas Tyr^{762} reached the maximal phosphorylation at 30 min instead of 5 min, as observed in the wild-type receptor. These data, summarized in Fig. 8, are consistent with our observations using phosphopeptide mapping (data not shown), indicating that the D849N mutation led to deregulated phosphorylation kinetics of certain tyrosine residues representing crucial binding sites for downstream molecular components of the PDGFRβ signaling.

Up-regulation of the Ras Pathway Downstream of the D849N Mutant PDGFRβ—PDGF is known to be a powerful mitogen for mesenchymal cells. An important pathway driving PDGFRβ-induced mitogenesis includes the Ras protein and the MAP kinase cascade. Upon ligand stimulation, Ras becomes activated via direct or indirect binding of the adaptor Grb2 in complex with the nucleotide exchange factor Sos to the activated PDGFRβ. This pathway is negatively controlled by RasGAP, which binds to phosphorylated Tyr^{770} in the kinase insert

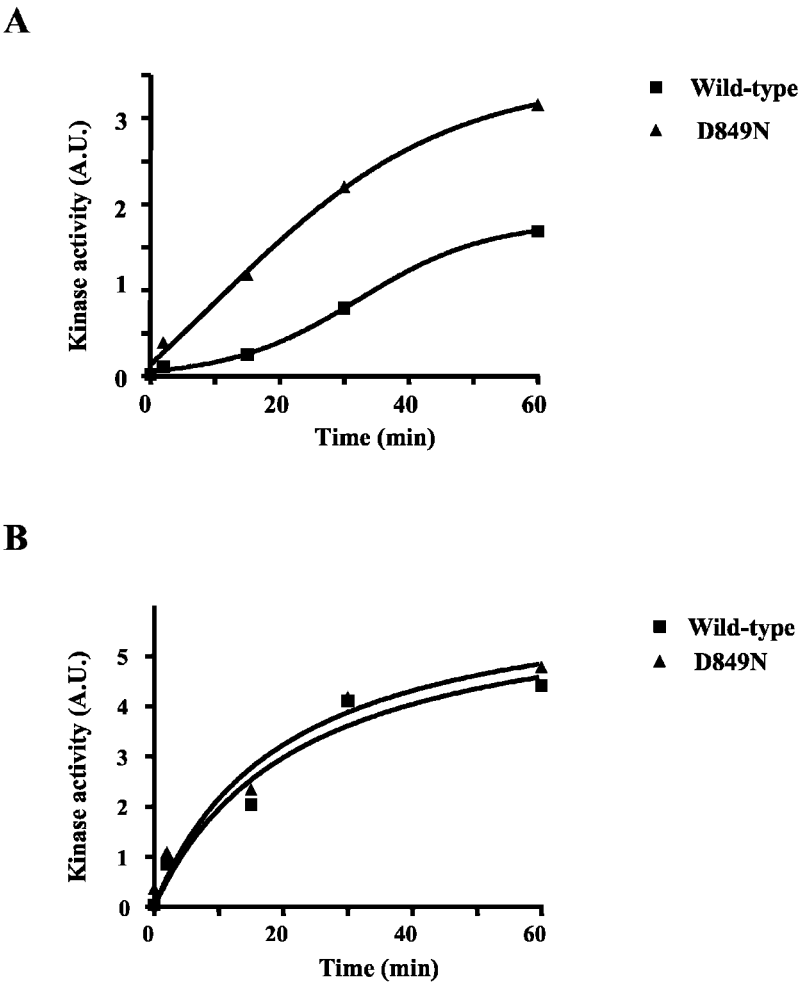

FIG. 5. **The activating mutation D849N increases the catalytic activity of the PDGFRβ toward an exogenous substrate.** Wild-type or mutant PDGFRβ was purified and prepared as described in the legend to Fig. 4. Unstimulated (*A*) or preactivated receptors (*B*) were incubated in the presence of [γ-^{32}P]ATP and the exogenous substrate myelin basic protein for increasing periods of time. The extent of exogenous substrate phosphorylation was determined by SDS-PAGE followed by analysis by PhosphorImager. Values were treated as described in the legend to Fig. 4.

of the receptor. Lack of interaction with RasGAP is correlated with an increased Ras activation and mitogenicity (24). In order to investigate the functional consequences of the changed phosphorylation kinetics in Tyr^{770} of the mutant receptor, we studied the physical association of RasGAP to wild-type and mutant receptor. We found that RasGAP associated with the wild-type receptor only very transiently following ligand stimulation (Fig. 9*A*), whereas in the case of mutant receptor, the association was increasing successively with stimulation time. These data were consistent with our previous finding of a delayed phosphorylation of the Tyr^{770} in ligand-induced D849N mutant PDGFRβ (Fig. 7*B*). In the next step, we wanted to investigate whether the changed interaction behavior between the mutant receptor and RasGAP had any functional consequences on Ras signaling. To monitor Ras activity, we examined the phosphorylation state of the well characterized downstream effector p44/p42 MAP kinase (ERK1/2). MAP kinase activation was analyzed by immunoblotting whole cell lysates from MEFs untreated or stimulated with PDGF-BB with antibodies against phosphorylated ERK1/2, followed by immunoblotting with anti-ERK1/2 antibodies to confirm an equal amount of protein (Fig. 9*B*). In the mutant cells, ERK1/2 was found to be phosphorylated at a low but significant level in the absence of ligand. In addition, upon ligand stimulation, ERK1/2 phosphorylation was more sustained in mutant cells compared with wild-type cells.

Finally, we tested the mitogenic response of wild-type and mutant MEFs toward PDGF-BB stimulation. Cells were stimulated with increasing amounts of PDGF-BB in the presence of [^{3}H]thymidine. The diagram in Fig. 9*C* shows that MEFs expressing D849N mutant PDGFRβ displayed an increased mitogenic response, compared with wild-type MEFs.

D849N Mutant PDGFRβ Constitutively Binds Phosphatidylinositol 3′-Kinase—Recent findings indicated that the PDGFRβ activates multiple signaling pathways that are involved in cellular transformation and that PI3K might be a key component by protecting cells from apoptosis (25). In addition, PI3K plays a central role in actin reorganization necessary for cellular migration and contraction (26).

Using site-selective, phosphospecific antibodies, we had already found that Tyr^{750}, one of the two PI3K binding sites on the PDGFRβ, was phosphorylated without ligand stimulation (Fig. 7*C*). We were interested to see whether this would also translate into changes in the interaction between PI3K and the mutant receptor. In coimmunoprecipitation experiments, we found a ligand-dependent association of the p85 regulatory subunit with the wild-type receptor, as described earlier (27). The mutant receptor, however, interacted constitutively with p85 (Fig. 10*A*) and thus could possibly initiate PI3K signaling even in the absence of ligand stimulation.

D849N Mutant PDGFRβ Constitutively Activates Protein Kinase B/Akt—In order to characterize the extent of PI3K signaling by the mutant PDGFRβ, we tested the phosphorylation status of protein kinase B/Akt, an important and well characterized mediator downstream of PI3K. As illustrated in Fig. 10*B*, phosphospecific antibodies able to recognize active Akt showed a ligand-inducible phosphorylation of this molecule in wild-type MEFs. In D849N mutant PDGFRβ MEFs, Akt was found to be constitutively phosphorylated, and the amount of phosphorylation could only be slightly increased by ligand

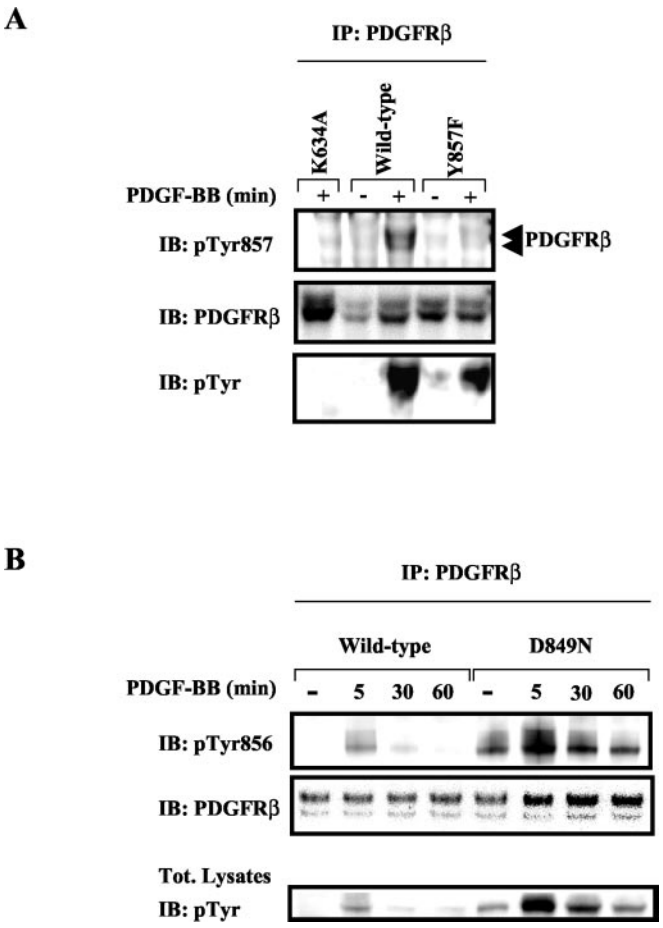

FIG. 6. **Constitutive phosphorylation of Tyr^{856} in the activation loop of mutant PDGFRβ.** *A*, lysates from COS cells transiently transfected with the indicated expression vectors were subjected to immunoprecipitation (*IP*) with anti-PDGFRβ antibodies. Immunoprecipitates were analyzed with phosphospecific antibodies raised against phosphorylated Tyr^{856} (Tyr^{857} in the human sequence) and anti-PDGFRβ. As a control, total lysates were subjected to immunoblotting (*IB*) with anti-phosphotyrosine. *K634A*, kinase-dead human PDGFRβ; *wild-type*, human wild-type PDGFRβ; *Y857F*, human PDGFRβ carrying phenylalanine in amino acid position 857 instead of tyrosine. *B*, lysates from MEFs expressing wild-type and D849N mutant PDGFRβ, stimulated with PDGF-BB for increasing time periods, were subjected to immunoprecipitation with anti-PDGFRβ antibodies. Immunoprecipitates were analyzed with phosphospecific antibodies against Tyr^{856} and antibodies against PDGFRβ. As a control, 20 μl of total lysates before immunoprecipitation were subjected to immunoblotting with anti-phosphotyrosine antibodies. One representative experiment out of two performed is shown.

stimulation. These results provide further evidence that PI3K is constitutively bound to and activated by the D849N mutant PDGFRβ even in the absence of ligand.

Apoptosis Protection Mediated by D849N Mutant PDGFRβ—As mentioned above, PI3K activity has a pivotal role in the control of cell survival, mainly through activation of the downstream serine/threonine kinase Akt (28). We reasoned that if D849N mutant PDGFRβ MEFs contain a constitutively activated PI3K and Akt, then these cells should be more resistant to apoptosis induction with respect to their wild-type counterparts. To perform a detailed investigation of the apoptosis response in wild-type and mutant MEFs, we assessed several independent apoptotic parameters with a cytofluorimetric approach (see "Experimental Procedures" and Ref. 17). As depicted in Fig. 10*C*, wild-type MEFs readily underwent apoptosis either when exposed to staurosporine, a prototypical death agonist, or when cultured in serum-depleted medium (Fig. 10*C*). As expected, D849N MEFs were much less sensitive to staurosporine, and only very little apoptosis could be triggered by serum starvation within 24 h (Fig. 10*C*). Only longer exposure to serum-free medium was able to activate an apoptotic program, but the kinetic was markedly slower in D849N than in wild-type MEFs (data not shown). Interestingly, in the presence of serum, the PI3K inhibitor LY294002 could not induce apoptosis *per se*, but it enhanced the effect of staurosporine (STS), in this way abolishing the differences recorded between D849N and wild-type MEFs (Fig. 10*C*).

The D849N Mutant PDGFRβ Mediates Cellular Motility in the Absence of Ligand—PI3K plays a pivotal role in mediating actin reorganization and motility responses (26). In order to investigate whether the constitutive activation of PI3K by the D849N mutant PDGFRβ causes an increased motility of the cells, we performed an *in vitro* "wound healing" assay. In this experiment, a "wound" was introduced into a confluent layer of MEFs that had been seeded on collagen-coated glass coverslips and starved overnight. Concomitant with wounding, the cells were either left unstimulated or stimulated with PDGF-BB or 10% fetal calf serum. In the presence of stimulation, both wild-type and mutant MEFs showed a strong tendency to close the wounds by migrating into the void space (Fig. 11). In the absence of stimulation, the wild-type cells showed no, or little, motility indicated by the clear and sharp wound edges even after 36 h. On the contrary, under these conditions, D849N mutant fibroblasts showed a strong tendency to migrate into the wounded area (Fig. 11). The difference in motility was also evident by the examination of filamentous actin in the cells. In the absence of ligand, mutant cells showed vivid edge ruffling activity, a prerequisite of migration, already after 2 h (Fig. 12); this biological effect was abolished in the presence of the PDGFRβ inhibitor (data not shown). In wild-type cells, edge ruffling was only observed after ligand or serum stimulation (Fig. 12).

DISCUSSION

Perturbation of RTK signaling by gain of function mutations results in deregulated kinase activity and is frequently associated with malignant transformation (22). In this paper, we have analyzed the biochemical mechanism and effects of an aspartic acid to asparagine mutation of codon 849 in the murine PDGFRβ. We found that mice homozygous for the D849N mutation are fertile and do not display any neoplastic phenotype for up to 12 months of age, whereas NIH3T3 fibroblasts expressing the D849N mutant PDGFRβ have transformed properties *in vitro* provided that stimulating ligand is present.

In order to find possible explanations of why the D849N mutant PDGFRβ displays transforming ability *in vitro* but not *in vivo*, we have compared the wild-type and the mutant PDGFRβs with respect to biochemical and signaling properties as well as cellular responses.

The kinetic parameters of the kinase activity are frequently found altered in receptors harboring point mutations in the activation loop. For instance, the homologous amino acid substitution (Asp → Asn) in the activation loop of the Met receptor lowers its threshold of activation, stabilizing an intermediate conformation close to the "open" one, characteristic of the fully active receptor. As a consequence, the mutant Met receptor becomes hyperphosphorylated and hyperactive (13). Similarly, our biochemical analysis has revealed that the amino acid substitution in the activation loop increases the overall tyrosine phosphorylation of the mutant PDGFRβ (Fig. 3*A*) as well as its sensitivity toward lower amounts of ligand. *In vitro* experiments showed that the introduction of the D849N mutation in the PDGFRβ does not cause full constitutive activation of the kinase *per se* but lowers the threshold for activation

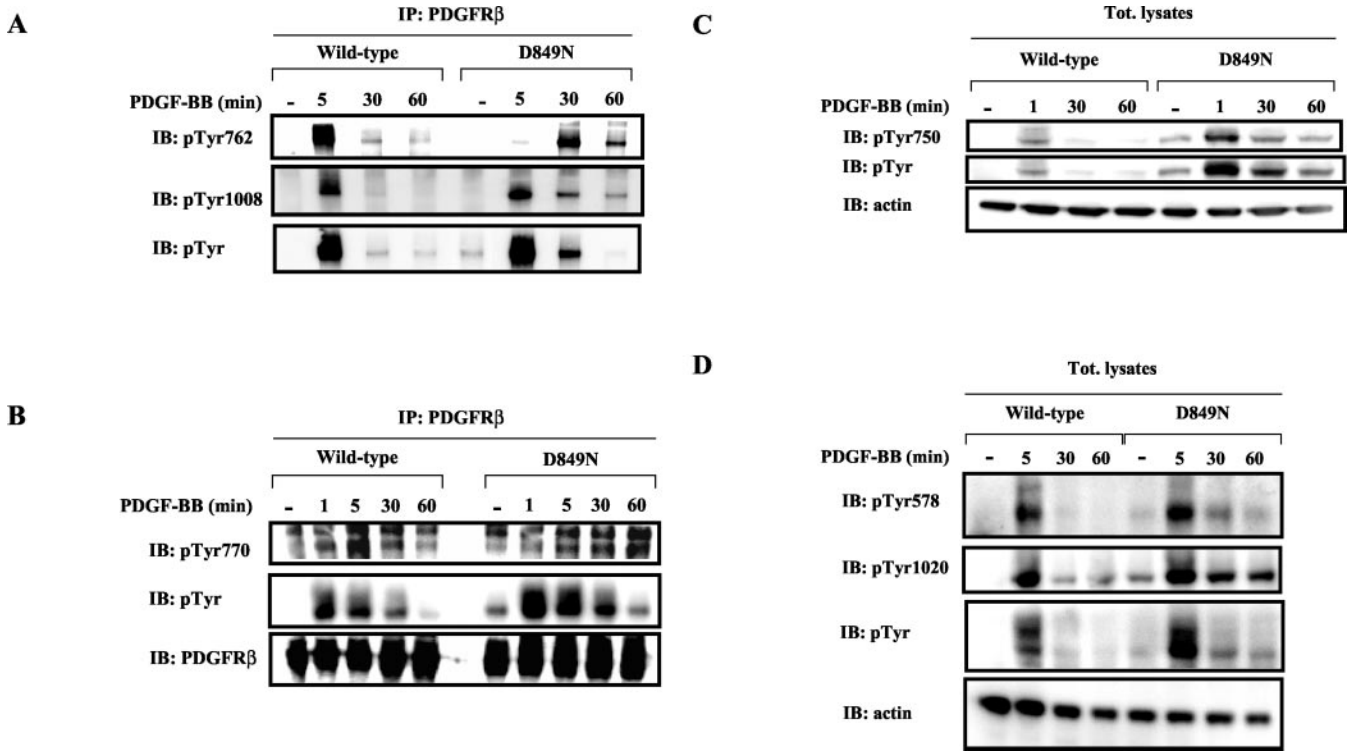

FIG. 7. **Deregulated phosphorylation of specific tyrosine residues in the D849N mutant PDGFRβ.** Wild-type or mutant PDGFRβ were immunoprecipitated (*IP*) from MEFs serum-starved for 48 h and stimulated with PDGF-BB for increasing time periods. Immunoprecipitated proteins were separated by SDS-PAGE, using a 4–12% gradient polyacrylamide gel and analyzed by Western blotting (*IB*) using antiphosphospecific antibodies against Tyr(P)^{762} and Tyr(P)^{1008} (*A*), Tyr(P)^{770} (*B*), Tyr(P)^{750} (*C*), and Tyr(P)^{578} and Tyr(P)^{1020} (*D*). Anti-PDGFRβ antibodies were used to determine the total amounts of PDGFRβ. Western blotting with anti-phosphotyrosine antibodies indicated the overall tyrosine phosphorylation of the PDGFRβ. Anti-actin immunoblotting was used to demonstrate equal protein concentrations in the different lysates.

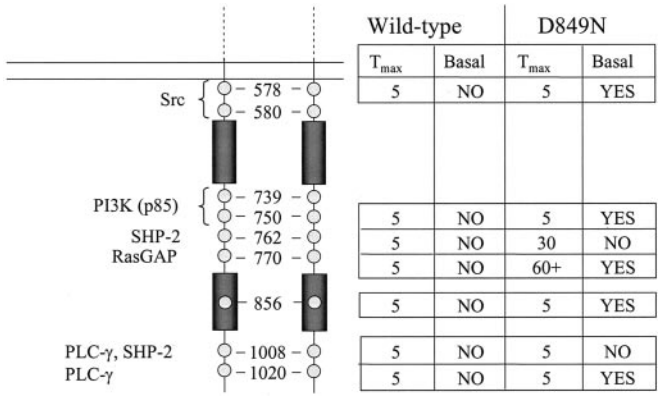

	Wild-type		D849N	
	T_{max}	Basal	T_{max}	Basal
Src	5	NO	5	YES
PI3K (p85)	5	NO	5	YES
SHP-2	5	NO	30	NO
RasGAP	5	NO	60+	YES
	5	NO	5	YES
PLC-γ, SHP-2	5	NO	5	NO
PLC-γ	5	NO	5	YES

FIG. 8. **Summary of the tyrosine phosphorylation kinetics for individual autophosphorylation sites in wild-type and D849N mutant PDGFRβ.** Overview of the phosphorylation differences between wild-type and D849N mutant PDGFRβs as established by the use of phosphorylation site-specific antibodies. T_{max}, time in minutes at which the phosphorylation maximum occurred in the time course performed; *Basal*, ligand-independent phosphorylation.

(Figs. 4 and 5). This finding might explain basal activity of the mutant receptor even after 2 days of starvation as well as the higher sensitivity of the mutant receptor. In agreement with the above observations, the major autophosphorylation site located in the activation loop of the PDGFRβ (Tyr^{856}) is phosphorylated in the unstimulated mutant receptor (Fig. 6*B*). We assume that a conformational change is induced by the presence of the mutation, which increases the chance of Tyr^{856} to become a substrate of an adjacent protomer and to activate the receptor, thus overcoming the need for stable receptor dimerization. Hence, we speculate that, as in the case of Met, the mutant PDGFRβ has a higher velocity of activation, compared with the wild-type receptor, but still needs ligand to achieve full activation.

The transforming activity triggered by receptor tyrosine kinases harboring a point mutation in the activation loop depends on the altered activation of downstream signaling molecules (29–31). Here, we undertook a detailed analysis linking changes in the phosphorylation of single receptor tyrosine residues with the activation of specific effector molecules. We have found that, in the mutant PDGFRβ, the binding sites for Src, PI3K, RasGAP, and phospholipase C-γ are phosphorylated in a ligand-independent fashion (Fig. 8). The Src binding sites are essential for the full activation of the PDGFRβ (23), since their phosphorylation is required for the removal of one of the inhibitory constraints controlling the PDGFRβ activity, located in the juxtamembrane domain of the receptor (32, 33).

The phosphorylation kinetics of the tyrosine residues acting as docking sites for the phosphatase SHP-2 and for RasGAP (Tyr^{762} and Tyr^{770}, respectively) (34) displayed a dramatic alteration in the mutant receptor, characterized by a significantly delayed peak of phosphorylation (Fig. 7, *A* and *B*). These differences in phosphorylation kinetics could be due to altered accessibility of these residues to specific kinases and/or phosphatases or altered activation patterns of specific kinases and/or phosphatases.

Furthermore, we observed that changes in the phosphorylation pattern of the receptor tyrosines directly translated into a deregulated recruitment of the cognate signal transducers, as exemplified by RasGAP and PI3K. RasGAP, which negatively regulates the Ras mitogenic pathway, displayed a successively increasing association with the mutant receptor, whereas the association to the wild-type receptor was seen only shortly after stimulation and very transiently (Fig. 9*A*). Interestingly, RasGAP was found to be tyrosine-phosphorylated with the corresponding kinetics in the respective cell lines (Supplemental

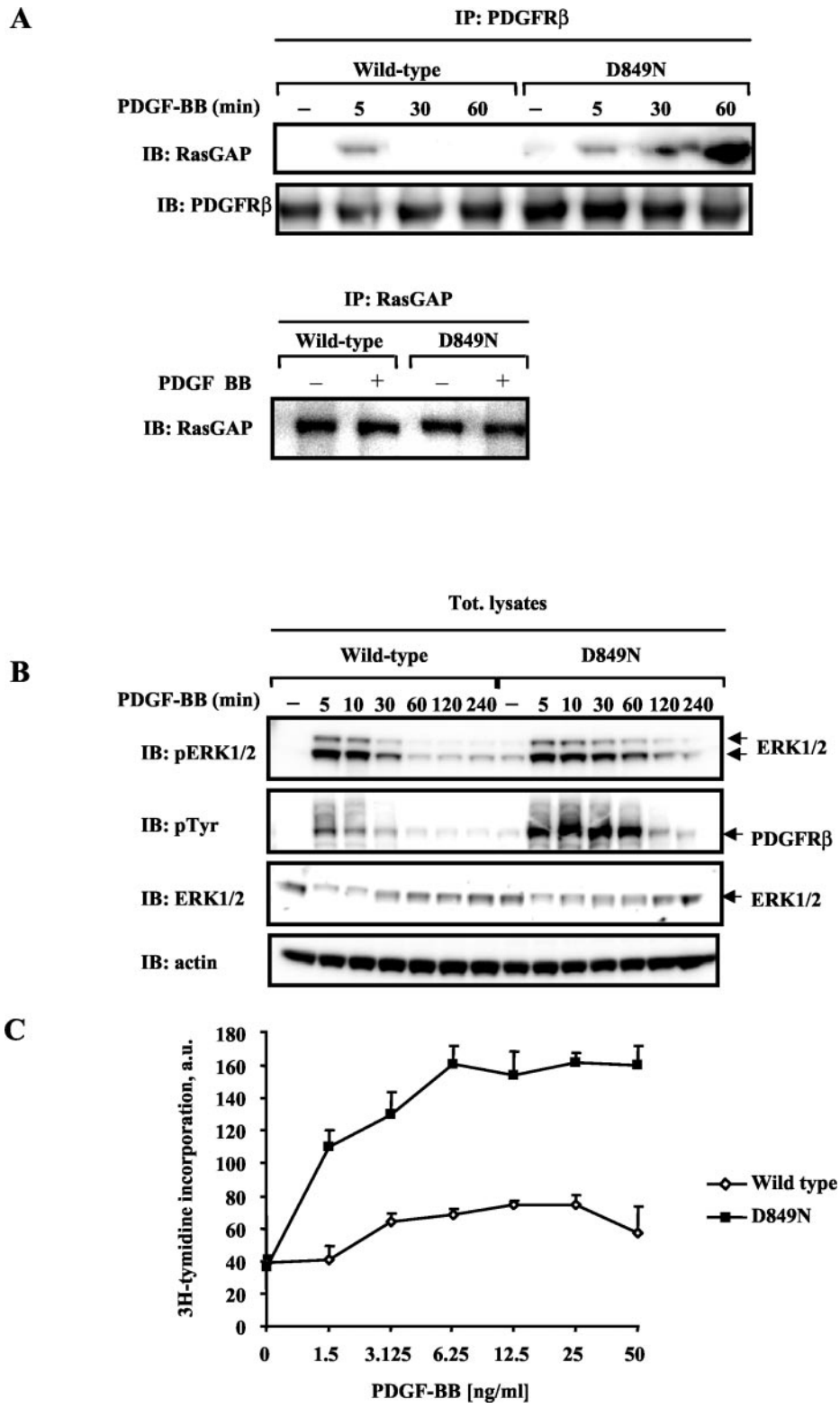

FIG. 9. **The D849N mutant PDGFRβ displays deregulated mitogenic signaling.** *A*, GTPase-activating protein for Ras (RasGAP) co-precipitated differently with activated D849N mutant PDGFRβ. MEFs expressing wild-type or D849N mutant PDGFRβ were serum-starved for 48 h and stimulated with PDGF-BB for increasing time periods. Wild-type or mutant PDGFRβ were immunoprecipitated (*IP*) and separated by SDS-PAGE, using a 4–12% gradient polyacrylamide gel. Co-precipitated RasGAP proteins were assayed by Western blotting (*IB*) using anti-RasGAP (*A*, *upper panel*). Immunoprecipitation of RasGAP was done to analyze the amount of total RasGAP expressed in the cells (*A*, *lower panel*). *B*, constitutive and prolonged phosphorylation of ERK1/2 MAP kinase in cells expressing D849N mutant PDGFRβ. MEFs expressing wild-type or D849N mutant PDGFRβ were stimulated with PDGF-BB for increasing time periods. Proteins from total lysates were separated by SDS-PAGE, using a 4–12% gradient polyacrylamide gel and analyzed by Western blotting with antibodies against ERK1/2, phospho-ERK1/2, and actin. *C*, increased mitogenic response to PDGF-BB of MEFs expressing D849N mutant PDGFRβ. MEFs expressing wild-type or D849N mutant PDGFRβ were serum-starved for 48 h and then incubated with [^{3}H]thymidine in the presence of the indicated amounts of PDGF-BB for 24 h at 37 °C. Incubation with 10% FCS was used as a positive control. For analysis, [^{3}H]thymidine radioactivity was precipitated using trichloroacetic acid, and the samples were measured in a scintillation counter. Data represent mean values of triplicates, including S.D. and are expressed relative to the [^{3}H]thymidine incorporation values obtained for stimulation with 10% fetal bovine serum.

Fig. 2). Lack of the RasGAP binding site on the PDGFRβ results in increased mitogenic signaling and mitogen-activated protein kinase activation (24). Intriguingly, the ERK/mitogen-activated protein kinase downstream of the D849N mutant PDGFRβ showed a higher and prolonged phosphorylation, and MEFs with mutant receptors showed increased proliferation upon ligand stimulation (Fig. 9, *B* and *C*). We have no plausible explanation for this apparent discrepancy, except that RasGAP could be trapped by the activated mutant receptor, such that it becomes excluded from its substrate, membrane-bound Ras. Due to the deregulated phosphorylation of the receptor, it is also possible that other effectors dominate ERK/mitogen-activated protein kinase signaling via other phosphorylation sites. Remarkably, the corresponding mutation in the Met receptor (*i.e.* D1228N) has been described to be transforming by preferential activation of the Ras pathway (30).

PI3K plays a central role in transduction pathways mediating different cellular responses, such as apoptosis protection and actin cytoskeletal reorganization (26, 28, 35). As mentioned earlier, the PI3K binding site in the D849N mutant

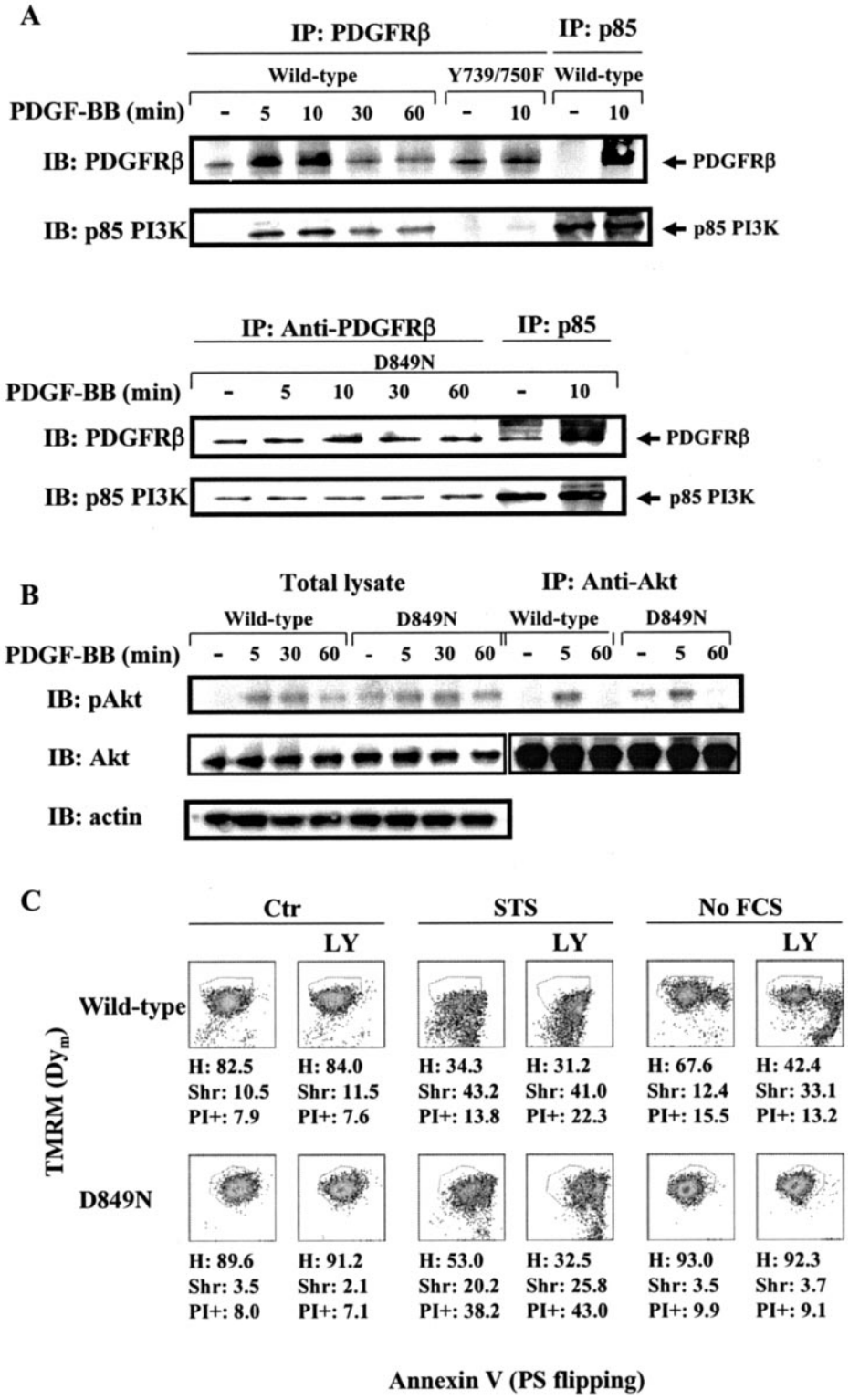

FIG. 10. **The PI3K signaling pathway is constitutively activated downstream of D849N mutant PDGFRβ.** *A*, constitutive binding of the p85 subunit of PI3K to the D849N mutant PDGFRβ. Lysates from MEFs expressing wild-type or D849N mutant PDGFRβ, stimulated with PDGF-BB for increasing time periods, were subjected to immunoprecipitation (*IP*) with anti-PDGFRβ or anti-p85 antibodies. As a negative control, immunoprecipitation with anti-p85 was performed using cell lysates from MEFs derived from knock-in mice with PDGFRβ unable to bind PI3K, due to mutation of the two autophosphorylation sites Tyr^{739} and Tyr^{750} (14). Immunoprecipitates were analyzed by immunoblotting (*IB*) using anti-PDGFRβ or anti-p85 antibodies. A representative experiment of three performed is shown. *B*, constitutive phosphorylation of Akt in D849N mutant MEFs. Lysates from MEFs expressing wild-type and D849N mutant PDGFRβ, stimulated with PDGF-BB for different time periods, were either separated directly or first subjected to immunoprecipitation with anti-Akt followed by immunoblotting with anti-phospho-Akt, anti-Akt, and anti-actin antibodies. *C*, increased Akt-dependent resistance to apoptosis of MEFs expressing D849N mutant PDGFRβ. Cells were exposed for 24 h to 25 ng/ml STS or were kept under starvation conditions (*No FCS*) to induce apoptosis. Where indicated, cells were incubated with the PI3K inhibitor LY294002 (*LY*; 20 μM). Apoptotic cells were scored using a fluorescence-activated cell sorter. Diagrams represent annexin V-fluorescein isothiocyanate (*i.e.* phosphatidylserine (*PS*) flipping across the plasma membrane) *versus* tetramethylrhodamine methyl ester staining (*i.e.* the measure of mitochondrial membrane polarity). Cells displaying mitochondrial depolarization, an early apoptotic hallmark, are shown in the *lower part* of each plot, whereas cells exposing PS on their surface, an intermediate apoptotic feature, are shown in the *right part* of the diagrams. Cells inside the selected area are viable cells, whose percentage is indicated by *H* (healthy). *Shr*, refers to shrunken cells, another intermediate apoptotic parameter. *PI+*, the percentage of propidium iodide-permeable (*i.e.* dead) cells. Both shrunken and propidium iodide-permeable cells were measured in the same experiment (plots not shown).

receptor was constitutively phosphorylated (Fig. 7*C*). This phosphorylation resulted in constitutive association with PI3K (Fig. 10*A*). Moreover, we found that the serine/threonine kinase Akt, downstream of PI3K, was activated by the mutant receptor even in the absence of ligand (Fig. 10*B*). This ligand-independent activation translated into an increased antiapoptotic signaling of serum-starved MEFs and an increased motility in cellular wounding assays in the absence of ligand (Figs. 10*C* and 11). In a mutant form of the Kit receptor, carrying a substitution of valine for aspartic acid in the corresponding codon (D816V) in the activation loop, PI3K is also constitutively bound and contributes to cellular transformation (36). Interestingly, however, in this case, Akt is only phosphorylated following ligand stimulation. Our findings indicate that the ligand-independent phosphorylation of the PI3K binding site (Tyr^{750}) activates the PI3K pathway and sustains its biological programs.

In summary, the D849N mutant PDGFRβ does not represent a fully constitutive active kinase but rather a deregulated enzyme with a lower threshold for activation. Signaling via the

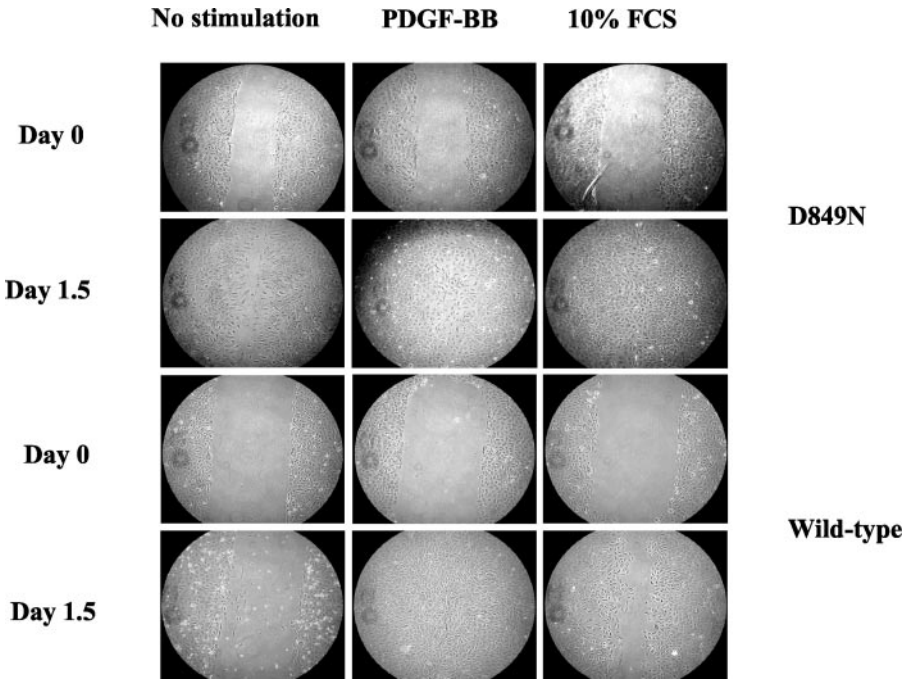

FIG. 11. **Increased ligand-independent migration of D849N mutant MEFs.** Wild-type or D849N mutant MEFs were plated on collagen-coated coverslips and serum-starved for 24 h. Concomitant with wounding, cells were either left unstimulated or were stimulated with PDGF-BB (20 ng/ml) or 10% fetal calf serum. After 36 h, photos were taken using a microscope with phase-contrast optics.

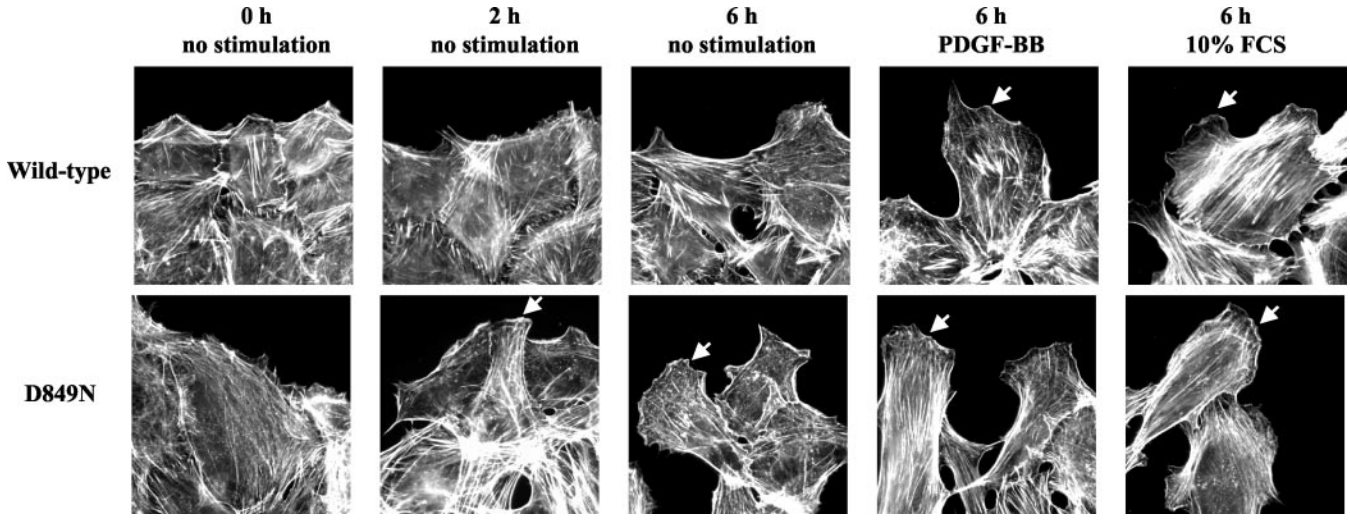

FIG. 12. **Actin reorganization in D849N mutant MEFs in the absence of ligand stimulation.** Wild-type or D849N mutant MEFs were plated on collagen-coated coverslips and either serum-starved, left untreated, or treated with PDGF-BB (20 ng/ml) or 10% FCS for the indicated time periods. Actin filaments were visualized with TRITC-labeled phalloidin.

mutant PDGFRβ is differently modulated by changes in tyrosine phosphorylation level and kinetics. This deregulates the activity and possibly also the localization of downstream molecules, like RasGAP and PI3K. Constitutively active PI3K signaling from the mutant receptor results in increased antiapoptotic signaling, which contributes to cellular transformation. However, the D849N mutant PDGFRβ is able to display its oncogenic potential only upon stimulation with PDGF-BB, as we have shown in the focus formation assay (Fig. 1). In this scenario, we can speculate that the mutation in the activation loop of the PDGFRβ provides an oncogenic predisposition and that other "hits" are required to achieve a fully transformed phenotype. This may explain why mutant mice have not developed tumors at the age of 1 year. Such a second hit could, for example, be sustained ligand stimulation. In order to test this exciting possibility, we are currently crossing a PDGF-B-transgene into the D849N mutant mice.

In conclusion, we provide evidence that a D849N mutation in the PDGFRβ affects the regulatory mechanism, ensuring a tight regulation of the kinase, and gives rise to a mutant receptor with a lower threshold for activation. In the presence of activating ligand, the mutant PDGFRβ displays abnormal autophosphorylation kinetics and consequently deregulates downstream signaling pathways leading to oncogenic conversion.

Acknowledgments—We thank Lena Claesson-Welsh and Lars Rönnstrand for generous donations of reagents and Paola Longati for critical reading of the manuscript. We are also grateful to Arne Östman and Camilla Persson for helpful discussion.

REFERENCES

1. Heldin, C. H., and Westermark, B. (1999) *Physiol. Rev.* **79,** 1283–1316
2. Pawson, T., and Scott, J. D. (1997) *Science* **278,** 2075–2080
3. Hubbard, S. R., and Till, J. H. (2000) *Annu. Rev. Biochem.* **69,** 373–398
4. Heldin, C. H., Östman, A., and Rönnstrand, L. (1998) *Biochim. Biophys. Acta* **1378,** 79–113
5. Rosenkranz, S., and Kazlauskas, A. (1999) *Growth Factors* **16,** 201–216
6. Heinrich, M. C., Corless, C. L., Duensing, A., McGreevey, L., Chen, C. J., Joseph, N., Singer, S., Griffith, D. J., Haley, A., Town, A., Demetri, G. D., Fletcher, C. D., and Fletcher, J. A. (2003) *Science* **299,** 708–710
7. Longley, B. J., Tyrrell, L., Lu, S. Z., Ma, Y. S., Langley, K., Ding, T. G., Duffy, T., Jacobs, P., Tang, L. H., and Modlin, I. (1996) *Nat. Genet.* **12,** 312–314

8. Nagata, H., Okada, T., Worobec, A. S., Semere, T., and Metcalfe, D. D. (1997) *Int. Arch. Allergy. Immunol.* **113,** 184–186
9. Tian, Q., Frierson, H. F., Jr., Krystal, G. W., and Moskaluk, C. A. (1999) *Am. J. Pathol.* **154,** 1643–1647
10. Yamamoto, Y., Kiyoi, H., Nakano, Y., Suzuki, R., Kodera, Y., Miyawaki, S., Asou, N., Kuriyama, K., Yagasaki, F., Shimazaki, C., Akiyama, H., Saito, K., Nishimura, M., Motoji, T., Shinagawa, K., Takeshita, A., Saito, H., Ueda, R., Ohno, R., and Naoe, T. (2001) *Blood* **97,** 2434–2439
11. Schmidt, L., Duh, F. M., Chen, F., Kishida, T., Glenn, G., Choyke, P., Scherer, S. W., Zhuang, Z., Lubensky, I., Dean, M., Allikmets, R., Chidambaram, A., Bergerheim, U. R., Feltis, J. T., Casadevall, C., Zamarron, A., Bernues, M., Richard, S., Lips, C. J., Walther, M. M., Tsui, L. C., Geil, L., Orcutt, M. L., Stackhouse, T., Lipan, J., Slife, L., Brauch, H., Decker, J., Niehans, G., Hughson, M. D., Moch, H., Storkel, S., Lerman, M. I., Linehan, W. M. and Zbar, B. (1997) *Nat. Genet.* **16,** 68–73
12. Schmidt, L., Junker, K., Weirich, G., Glenn, G., Choyke, P., Lubensky, I., Zhuang, Z., Jeffers, M., Vande Woude, G., Neumann, H., Walther, M., Linehan, W. M., and Zbar, B. (1998) *Cancer Res.* **58,** 1719–1722
13. Chiara, F., Michieli, P., Pugliese, L., and Comoglio, P. M. (2003) *J. Biol. Chem.* **278,** 29352–29358
14. Heuchel, R., Berg, A., Tallquist, M., Ahlen, K., Reed, R. K., Rubin, K., Claesson-Welsh, L., Heldin, C. H., and Soriano, P. (1999) *Proc. Natl. Acad. Sci. U. S. A.* **96,** 11410–11415
15. Nagy, A., Rossant, J., Nagy, R., Abramow-Newerly, W., and Roder, J. C. (1993) *Proc. Natl. Acad. Sci. U. S. A.* **90,** 8424–8428
16. Wood, S. A., Allen, N. D., Rossant, J., Auerbach, A., and Nagy, A. (1993) *Nature* **365,** 87–89
17. Tallquist, M. D., Klinghoffer, R. A., Heuchel, R., Mueting-Nelsen, P. F., Corrin, P. D., Heldin, C. H., Johnson, R. J., and Soriano, P. (2000) *Genes Dev.* **14,** 3179–3190
18. Todaro, G. J., and Green, H. (1963) *J. Cell Biol.* **17,** 299–313
19. Persson, C., Savenhed, C., Bourdeau, A., Tremblay, M. L., Markova, B., Bohmer, F. D., Haj, F. G., Neel, B. G., Elson, A., Heldin, C. H., Ronnstrand, L., Ostman, A., and Hellberg, C. (2004) *Mol. Cell. Biol.* **24,** 2190–2201
20. Rasola, A., and Geuna, M. (2001) *Cytometry* **45,** 151–157
21. Bardelli, A., Longati, P., Gramaglia, D., Basilico, C., Tamagnone, L., Giordano, S., Ballinari, D., Michieli, P., and Comoglio, P. M. (1998) *Proc. Natl. Acad. Sci. U. S. A.* **95,** 14379–14383
22. Blume-Jensen, P., and Hunter, T. (2001) *Nature* **411,** 355–365
23. Baxter, R. M., Secrist, J. P., Vaillancourt, R. R., and Kazlauskas, A. (1998) *J. Biol. Chem.* **273,** 17050–17055
24. Ekman, S., Thuresson, E. R., Heldin, C. H., and Ronnstrand, L. (1999) *Oncogene* **18,** 2481–2488
25. DeMali, K. A., Whiteford, C. C., Ulug, E. T., and Kazlauskas, A. (1997) *J. Biol. Chem.* **272,** 9011–9018
26. Hawkins, P. T., Eguinoa, A., Qiu, R. G., Stokoe, D., Cooke, F. T., Walters, R., Wennstrom, S., Claesson-Welsh, L., Evans, T., Symons, M., and Stephens, L. (1995) *Curr. Biol.* **5,** 393–403
27. Kazlauskas, A., and Cooper, J. A. (1990) *EMBO J.* **9,** 3279–3286
28. Kauffmann-Zeh, A., Rodriguez-Viciana, P., Ulrich, E., Gilbert, C., Coffer, P., Downward, J., and Evan, G. (1997) *Nature* **385,** 544–548
29. Piao, X., and Bernstein, A. (1996) *Blood* **87,** 3117–3123
30. Giordano, S., Maffe, A., Williams, T. A., Artigiani, S., Gual, P., Bardelli, A., Basilico, C., Michieli, P., and Comoglio, P. M. (2000) *FASEB J.* **14,** 399–406
31. De Vita, G., Melillo, R. M., Carlomagno, F., Visconti, R., Castellone, M. D., Bellacosa, A., Billaud, M., Fusco, A., Tsichlis, P. N., and Santoro, M. (2000) *Cancer Res.* **60,** 3727–3731
32. Chiara, F., Bishayee, S., Heldin, C. H., and Demoulin, J. B. (2004) *J. Biol. Chem.* **279,** 19732–19738
33. Irusta, P. M., Luo, Y., Bakht, O., Lai, C. C., Smith, S. O., and DiMaio, D. (2002) *J. Biol. Chem.* **277,** 38627–38634
34. Ekman, S., Kallin, A., Engstrom, U., Heldin, C. H., and Ronnstrand, L. (2002) *Oncogene* **21,** 1870–1875
35. Vanhaesebroeck, B., Leevers, S. J., Panayotou, G., and Waterfield, M. D. (1997) *Trends Biochem. Sci.* **22,** 267–272
36. Chian, R., Young, S., Danilkovitch-Miagkova, A., Ronnstrand, L., Leonard, E., Ferrao, P., Ashman, L., and Linnekin, D. (2001) *Blood* **98,** 1365–1373